Resilient Distribution System by Microgrids Formation After Natural Disasters

Chen Chen, *Member, IEEE*, Jianhui Wang, *Senior Member, IEEE*, Feng Qiu, *Member, IEEE*, and Dongbo Zhao, *Member, IEEE*

***Abstract*—Microgrids with distributed generation (DG) provide a resilient solution in the case of major faults in a distribution system due to natural disasters. This paper proposes a novel distribution system operational approach by forming multiple microgrids energized by DG from the radial distribution system in real-time operations to restore critical loads from the power outage. Specifically, a mixed-integer linear program is formulated to maximize the critical loads to be picked up while satisfying the self-adequacy and operation constraints for the microgrids formation problem by controlling the ON/OFF status of the remotely controlled switch devices and DG. A distributed multiagent coordination scheme is designed via local communications for the global information discovery as inputs of the optimization, which is suitable for autonomous communication requirements after the disastrous event. The formed microgrids can be further utilized for power quality control and can be connected to a larger microgrid before the restoration of the main grids is complete. Numerical results based on modified IEEE distribution test systems validate the effectiveness of our proposed scheme.**

***Index Terms*—Distribution system, microgrids, mixed-integer linear program (MILP), multiagent coordination, resilience.**

I. Introduction

RECENT severe power outages caused by natural disasters, such as floods and hurricanes, have highlighted the importance and urgency to improve grid resilience of the U.S. For example, Hurricane Sandy left approximately 7.5 million customers without power across 15 states and Washington, DC, after it hit the eastern shore of the U.S. [1]. A recent Congressional Research Service study estimates the inflation-adjusted cost of weather-related outages at $25 to $70 billion annually in the U.S. [2]. Grid resilience is increasingly critical since the number of outages caused by severe weather is expected to rise as climate change increases the frequency and intensity of hurricanes, blizzards, floods, and other extreme weather events [3]. As the utility grids remain quite vulnerable and exposed to natural disasters, rather than protecting the power grids from storms like Sandy, the power industry has focused on methods of restoring the distribution system quickly after disasters to achieve resilient power grids [1].

Distribution system restoration, which aims to restore loads after a fault by altering the topological structure of the distribution network, has been extensively studied in the literature using various methodologies, including expert systems [4], [5], fuzzy logic [6], [7], multiagent systems [8], [9], heuristic search [10], and optimization [11]. These methods can effectively isolate the fault and restore as much load as possible after the general blackout in the distribution system. However, when facing natural disasters like super storm Sandy, the substations may be at fault so that the distribution system cannot be supplied by the main grids, or the damages to the distribution facilities cause isolated areas without power. In these scenarios, traditional distribution system restoration approaches cannot guarantee that energy will continue to be supplied to customers after natural disasters.

The distributed generation (DG) units managed by microgrids provide an alternative approach to continue supplying critical loads after major faults of the main grids [12]. DGs such as fossil-fuel-based combustion generators have been widely used as backup generators (or standby generators) to supply the load in a building after the outage [13]. With the emerging smart grid technology, many electric distribution utilities are planning to implement remotely controlled automatic switch devices on distribution feeders as part of their grid modernization strategy to achieve the vision of a "self-healing" distribution grid (see distribution automation programs in [14]). These automatic switch devices make it possible to expand supply coverage of the backup DG beyond its adjacent building to restore more critical loads, i.e., forming a microgrid for load restoration. However, how to efficiently form microgrids from several DGs in the distribution system is not an easy task, especially in the case of facilities being destroyed due to a disaster. In addition, the communication requirements in the presence of disastrous events create more challenges for the restoration.

To tackle these challenges, we propose a microgrids formation scheme to restore critical loads in a radial distribution system after major faults at the main grid as a result of a natural disaster. Based on recent industry trends that more and more remotely controlled automatic switch facilities are being implemented by electric utilities, DGs are

Manuscript received January 20, 2015; revised April 17, 2015; accepted April 30, 2015. This work was supported by the U.S. Department of Energy Office of Electricity Delivery and Energy Reliability. Paper no. TSG-00064-2015.

C. Chen, J. Wang, and F. Qiu are with the Energy Systems Division, Argonne National Laboratory, Argonne, IL 60439 USA (e-mail: morningchen@anl.gov; jianhui.wang@anl.gov; fqiu@anl.gov).

D. Zhao is with Eaton Corporation, Eden Prairie, MN 55344 USA (e-mail: dongbozhao@eaton.com).

Color versions of one or more of the figures in this paper are available online at http://ieeexplore.ieee.org.

Digital Object Identifier 10.1109/TSG.2015.2429653

 h the exception of pagination.

exploited to restore more loads via a microgrid instead of just continuing to supply the nearby load. Specifically, by controlling the ON/OFF status of the automatic switch devices, each microgrid, which is energized by a DG, is formed separately. The microgrids formation problem is formulated as a mixed-integer linear program (MILP) to maximize the total prioritized loads to be picked up while satisfying the self-adequacy, topology, and operation constraints. To cope with the resilience challenge of communications after a natural disaster, we design the global information discovery for the optimization as a distributed multiagent coordination via only local communications by applying the average consensus algorithm. Case studies based on modified IEEE distribution test systems were conducted to validate the proposed approach.

Several works in the literature discuss using microgrids for the distribution service restoration (see [12], [15]–[20]). In [15] and [17], a sequence of operation principles for the microgrids in an emergency operation mode after the blackout is investigated, and control algorithms are discussed to reduce restoration time. Castillo [16] developed a stochastic MILP to access the impact of coordinating microgrids as a blackstart resource after a natural disaster. These works are based on a scenario that requires the microgrids to be installed beforehand, which may not be available at the current stage. Our approach instead forms the microgrids dynamically after the disaster happens by utilizing the automatic switch facilities and DG units. Li *et al.* [18] modeled the microgrids as virtual feeders and apply the spanning tree search to maximize the restored load and minimize the number of switching operations. However, the approach is only for a single fault, which is not suitable for the restoration after the disastrous event. Pham *et al.* [12] and Wang and Wang [19] proposed a restoration method utilizing the dispersed generation insertion. However, this paper, as well as the other works discussed above, does not consider the communication requirements for the restoration after the disaster. Xu and Liu [20] proposed a multiagent coordination for distributed information discovery, but the restoration process does not consider the topology of the distribution network. To the best of our knowledge, this paper is the first to propose dynamically forming microgrids to continue supplying critical loads after a disastrous event to achieve a resilient distribution system.

The remainder of this paper is organized as follows. Section II describes the microgrids formation problem to restore critical loads after major faults at the main grid. Section III formulates the MILP for the microgrids formation optimization. Section IV proposes the global information discovery scheme for the optimization via average consensus algorithms. Section V provides numerical results to validate our approach, and we conclude in Section VI.

II. Problem Formulation

We consider a radial power distribution system consisting of N nodes denoted by the set of nodes $\mathcal{N} := \{1, \ldots, N\}$, and L power lines represented by the set of edges $\mathcal{L} := \{(i, j)\} \subseteq \mathcal{N} \times \mathcal{N}$.[1] At each node $i \in \mathcal{N}$, there is a load that has the demand of real and reactive power, denoted by p_i and q_i, respectively. When there is a major fault at the main grids as a result of a natural disaster, the distribution system can no longer be energized by the main grids through the substation and feeders. Instead, the DGs installed at certain nodes, which are denoted by the set $\mathcal{G} \subset \mathcal{N}$, can be utilized to continue supplying critical loads in the distribution system before the restoration of the main grids is complete. To achieve this goal, we have made three assumptions in this paper.

1) Rather than acting as a backup generator just supplying the load at node $i \in \mathcal{G}$, we assume that the DG can expand its coverage to supply multiple loads by separately forming K microgrids, the set of which is denoted by $\mathcal{K}$. This assumption is from the fact that the value of microgrids with DGs to achieve grid resilience has been recognized, and they are being adopted by some state governments and industries, and their technical, regulatory, and financial barriers for implementations are being studied [22], [23]. Under this assumption, each microgrid $k \in \mathcal{K}$ consists of a set of nodes $\mathcal{N}_k$ satisfying $\mathcal{N}_k \subset \mathcal{N}$ and $\mathcal{N}_{k_1} \cap \mathcal{N}_{k_2} = \varnothing$, $\forall k_1, k_2 \in \mathcal{K}$. Each microgrid is energized by a DG, so we get $|\mathcal{K}| = |\mathcal{G}| = K$. For notational simplicity, we define the set of microgrids $\mathcal{K}$ the same as the set of nodes where DGs are installed, i.e., $\mathcal{K} \triangleq \mathcal{G}$.
2) The remotely controlled automatic switch devices are assumed to be available in the distribution network so that lines can be opened/closed and loads can be connected/disconnected to form multiple microgrids. This assumption is reasonable due to the fact that with fast development of distribution automation technology, the remotely controlled automatic switch devices are being implemented on distribution feeders by many utilities [14], e.g., the Spokane Smart Circuit project by Avista Utilities [24]. Depending on the distribution automation progress, these remotely controlled automatic switch devices (for ease of description, we use the term "switch" throughout this paper) can be fully or partly installed at each line and node, to provide different flexibilities in controlling the topology of the distribution network. In addition, due to the natural disaster, some switches may be at fault. Our approach can easily accommodate these cases as described in Section III-A6. Based on the assumption, let $c_{ij} \in \{0, 1\}$ denote the binary decision variables indicating whether the switch associated with line (i, j) is open ($c_{ij} = 0$) or closed ($c_{ij} = 1$). Similarly, let $s_i \in \{0, 1\}$ denote the binary decision variables representing whether the switch connecting the load and node i is open ($s_i = 0$) or closed ($s_i = 1$). By controlling these switches, K self-adequate microgrids are formed to maximize the total critical

[1] We consider the radial topology in this paper because the majority of distribution systems are configured as a radial network. For the advanced network topology other than radial (see [21]), the formulation needs modifications and it is left for future research.

 h the exception of pagination.

loads to be restored. In Section III, we describe the optimization formulation for this problem in detail.

3) The switches are assumed to have local communication capabilities to exchange information with its neighboring switches, which can be achieved by utilizing the matured short-range low-cost wireless networks like Wi-Fi or ZigBee. The communication network enables effective collection of the operation parameters of the distribution system (e.g., power demand values of all nodes, distribution network topology information) as inputs for the controller to make decisions of forming multiple microgrids at the time of the restoration. This process is called the global information discovery [20]. Unlike the centralized approach that presents significant challenges to the resilience of the communication infrastructure during and after a disastrous event, we design the distributed multiagent coordination for the global information discovery based on the distributed communication network assumed, which is suitable for the dynamic features of the communications regarding a disastrous event. In Section IV, we discuss the multiagent coordination scheme for the global information discovery.

III. Microgrids Formation in Radial Distribution System

In this section, the optimization for microgrids formation in the distribution system is presented. K microgrids, each with one DG, are formed by controlling the switches and output of DGs by solving the MILP problem, to maximize the total critical loads to be restored after the natural disaster, and to guarantee that each microgrid is a self-adequate system.

A. Constraints for Microgrids Formation in MILP

1) Node Clustering Constraints (NCC): If the load at node $i \in \mathcal{N}$ can be energized by microgrids, this node can only belong to one of the K microgrids. However, some nodes may stay islanded without being connected to any microgrid due to permanent line faults. To tackle this issue, these faulted islands should be removed from the set of nodes $\mathcal{N}$ to model the node clustering constraints. This can be achieved by finding the connected components of an undirected graph representing the distribution system topology and removing the nodes and edges of the connected component without a DG. For the preprocessed radial distribution network, the set of nodes and edges are denoted by $\bar{\mathcal{N}}$ and $\bar{\mathcal{L}}$, respectively.

Define auxiliary binary decision variables $v_{ik} \in \{0, 1\}$ indicating whether node $i \in \bar{\mathcal{N}}$ belongs to microgrid $k \in \mathcal{K}$ ($v_{ik} = 1$ if node i belongs to microgrid k, and $v_{ik} = 0$ otherwise), and the node clustering constraints can be expressed as

$$\sum_{k \in \mathcal{K}} v_{ik} = 1, \ \forall i \in \bar{\mathcal{N}}. \tag{1}$$

For node i at which the DG k is installed, i.e., $i = k$, node i will surely belong to microgrid k, which can be written as the following equality constraints:

$$v_{ik} = 1, \ i = k, \ \forall i \in \bar{\mathcal{N}}, \ k \in \mathcal{K}. \tag{2}$$

2) Microgrid Connectivity Constraints (MCC): For a radial (tree) distribution network, each microgrid can be viewed as a subtree network with the root node being the node where the DG is installed. Due to the connectivity feature of a tree, one node can belong to microgrid k only if its parent node (for this microgrid) belongs to microgrid k, which can be expressed as the following inequality constraints:

$$v_{ik} \le v_{jk}, \ \forall k \in \mathcal{K}, i \in \bar{\mathcal{N}} \setminus \{k\}, j = \theta_k(i) \tag{3}$$

where $\theta_k(i)$ denotes the parent node of node i regarding microgrid k.

3) Microgrid Branch-Node Constraints (MBNC): Next we consider the constraints with respect to the relation between nodes and lines in a microgrid. We see that if both nodes i and j belong to microgrid k, i.e., $v_{ik} = v_{jk} = 1$, then the line connecting nodes i and j should also belong to microgrid k. Together with (3), we can further derive that if the children node of (i, j) (regarding microgrid k) belong to this microgrid, then line (i, j) belongs to microgrid k. If line (i, j) belongs to any one of the microgrid in $\mathcal{K}$, the switch on this line (if it exists) should be in the closed state. Thus, the branch-node constraints can be expressed as

$$c_{ij} = \sum_{k \in \mathcal{K}} v_{hk}, \ h = \zeta_k(i, j), \ (i, j) \in \bar{\mathcal{L}} \tag{4}$$

where $h = \zeta_k(i, j)$ denotes the children node of line (i, j) regarding microgrid k.

4) Microgrid Load Pickup Constraints (MLPC): If the load at node i can be energized by microgrid $k \in \mathcal{K}$, the following two conditions should be satisfied simultaneously: 1) node i belongs to microgrid k, i.e., $v_{ik} = 1$ and 2) the switch associated with the load is closed so that the load is connected to node i, i.e., $s_i = 1$. These two conditions can be written in a uniform manner as $v_{ik} \cdot s_i = 1$, which is a quadratic constraint. To address this nonlinearity issue, define the auxiliary binary decision variables $\gamma_{ik} \in \{0, 1\}$ as: $\gamma_{ik} = v_{ik} \cdot s_i, \forall i \in \bar{\mathcal{N}}, k \in \mathcal{K}$, and the quadratic equality constraints can be further converted to the following three linear inequality constraints:

$$\gamma_{ik} \le v_{ik}, \ \forall i \in \bar{\mathcal{N}}, \ k \in \mathcal{K} \tag{5}$$

$$\gamma_{ik} \le s_i, \ \forall i \in \bar{\mathcal{N}}, \ k \in \mathcal{K} \tag{6}$$

$$\gamma_{ik} \ge v_{ik} + s_i - 1, \ \forall i \in \bar{\mathcal{N}}, \ k \in \mathcal{K}. \tag{7}$$

5) Microgrid Operation Constraints (MOC): The microgrids formation should also satisfy operation constraints, e.g., power balance and voltage limit at each node. The DistFlow model in [25] can be used as the power flow model for the radial network, i.e., each microgrid. In addition, we apply linearized approximation of DistFlow model [26] to formulate microgrid operation constraints. Specifically, let P_i^k and Q_i^k denote the real and reactive power flow into node i for microgrid k. Since each microgrid is of a tree topology with DG at the root node, each node has only one in-flow power, as shown in Fig. 1.

 h the exception of pagination.

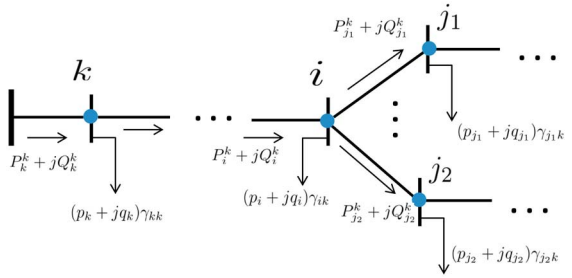

Fig. 1. DistFlow model for radial distribution network regarding microgrid k.

According to the linearized DistFlow model [26], the real and reactive power balance at each node for microgrid k can be written as

$$\sum_{j\in\mathcal{S}_i^k} P_j^k = P_i^k - \gamma_{ik}\cdot p_i,\ \ \forall k\in\mathcal{K}, i\in\bar{\mathcal{N}} \tag{8}$$

$$\sum_{j\in\mathcal{S}_i^k} Q_j^k = Q_i^k - \gamma_{ik}\cdot q_i,\ \ \forall k\in\mathcal{K}, i\in\bar{\mathcal{N}} \tag{9}$$

where $\mathcal{S}_i^k$ denote the set of children nodes of node i for microgrid k. Note that if node i does not belong to microgrid k (i.e., $v_{ik}=0$), the real and reactive in-flow power regarding microgrid k (i.e., P_i^k and Q_i^k) should be zero, which can be described by the following inequality constraints:

$$0\le P_i^k \le v_{ik}\cdot P_k^{\max},\ \ \forall k\in\mathcal{K}, i\in\bar{\mathcal{N}} \tag{10}$$

$$0\le Q_i^k \le v_{ik}\cdot Q_k^{\max},\ \ \forall k\in\mathcal{K}, i\in\bar{\mathcal{N}} \tag{11}$$

where $P_k^{\max}$ and $Q_k^{\max}$ denote the capacity of the DG in microgrid k. We can see from (10) and (11) that the in-flow power of DG nodes, which are denoted by P_k^k and Q_k^k, is within the capacity of the corresponding DG, i.e., $0\le P_k^k\le P_k^{\max}$ and $0\le Q_k^k\le Q_k^{\max}$. Note that the adjustable reactive power Q_k^k is provided by DG k. In addition, the capacitor banks installed on the feeders also provide reactive power of fixed values, and the reactive power demand q_i at node i has already deducted the reactive power injection by capacitor banks at this node.

For the voltage constraints, the voltage at DG nodes will be set to the reference values, denoted by V_0^k for microgrid k. According to the linearized DistFlow model, the voltages at other nodes regarding microgrid k, which are denoted by V_i^k, can be expressed as

$$V_i^k = V_j^k - \frac{r_i P_i^k + x_i Q_i^k}{V_0^k} - \delta_i^k, j=\theta_k(i), i\in\bar{\mathcal{N}}\setminus\{k\}, k\in\mathcal{K} \tag{12}$$

where r_i and x_i denote the resistance and reactance of line (i,j). Note that V_i^k should be less than V_0^k if node i belongs to microgrid k; otherwise V_i^k should be zero. This condition can be written as the following inequality constraints:

$$0\le V_i^k \le v_{ik}\cdot V_0^k,\ \ \forall k\in\mathcal{K}, i\in\bar{\mathcal{N}}. \tag{13}$$

The δ_i^k in (12) is a slack variable to make the equality constraint valid when node i does not belong to microgrid k but its parent node j belongs to microgrid k. The constraints for δ_i^k can be written as

$$0\le \delta_i^k \le (1-v_{ik})\cdot V_0^k,\ \ \forall k\in\mathcal{K}, i\in\bar{\mathcal{N}}. \tag{14}$$

With V_i^k for microgrid k, the actual voltage at node i can be expressed as $\sum_{k\in\mathcal{K}} V_i^k$. This voltage should be within a range specified by the rated voltage V_R and tolerance ϵ, that is

$$V_R - \epsilon\cdot V_R \le \sum_{k\in\mathcal{K}} V_i^k \le V_R + \epsilon\cdot V_R,\ \ \forall i\in\bar{\mathcal{N}}. \tag{15}$$

6) Distribution System Condition Constraints (DSCC): Due to the disastrous event, some lines may be at fault (i.e., the lines are in the open state) and the repairs need a substantial amount of time, or some switches fail and are in the open state. In this case, denote these lines by the set $\mathcal{L}_O$, and we can write the constraints as $c_{ij}=0,\ \forall(i,j)\in\mathcal{L}_O\subset\bar{\mathcal{L}}$. On the other hand, some lines may have fault switches which are in the closed state. These lines, denoted by the set $\mathcal{L}_C\subset\bar{\mathcal{L}}$, can be treated as always in the closed state, i.e., $c_{ij}=1$, $\forall(i,j)\in\mathcal{L}_C\subset\bar{\mathcal{L}}$. Similar distribution system condition constraints can be applied to the switches at nodes where $\mathcal{N}_O$ denotes the set of fault switches that separate the load from the node permanently, and $\mathcal{N}_C$ denotes the set of loads that are with fault switches in the closed state and must be always connected to the node. The constraints regarding the binary decision variables based on the actual conditions of the distribution system can be written as follows:

$$c_{ij}=0,\ \ \forall(i,j)\in\mathcal{L}_O \tag{16}$$

$$c_{ij}=1,\ \ \forall(i,j)\in\mathcal{L}_C \tag{17}$$

$$s_i=0,\ \ \forall i\in\mathcal{N}_O \tag{18}$$

$$s_i=1,\ \ \forall i\in\mathcal{N}_C. \tag{19}$$

B. Optimization Formulation

In general, loads have priorities to be picked up with regard to their importance to sustaining critical functions. For example, hospitals will be more crucial than those of the entertainment sector. So for the load restoration after the blackout due to a natural disaster, these significant loads should be given higher priorities. Let w_i denote the priority weight associated with the load at node i, and a larger value of w_i indicates higher priority. The total priority weighted load picked up can be expressed as $\sum_{i\in\bar{\mathcal{N}}} w_i \sum_{k\in\mathcal{K}}\gamma_{ik}\cdot p_i$. The microgrids formation optimization aims to maximize the total priority weighted loads picked up, subject to the constraints discussed above, which can be expressed as an MILP problem[2]

$$\max_{s_i,c_{ij},v_{ik},\gamma_{ik},P_i^k,Q_i^k,V_i^k,\delta_i^k}\ \ \sum_{i\in\bar{\mathcal{N}}} w_i\cdot\sum_{k\in\mathcal{K}}\gamma_{ik}\cdot p_i \tag{20}$$

$$\text{s.t.}\ \ \text{NCC: (1), (2)} \tag{21}$$

$$\text{MCC: (3)} \tag{22}$$

$$\text{MBNC: (4)} \tag{23}$$

$$\text{MLPC: (5)–(7)} \tag{24}$$

$$\text{MOC: (8)–(15)} \tag{25}$$

$$\text{DSCC: (16)–(19)} \tag{26}$$

[2]In this paper, we assume that loads are of fixed values requested by the loads for the microgrids formation. However, after the microgrids are formed, these loads may vary during the operation. To cope with this variation, the fixed values requested by the loads can be their maximum demands to assure adequacy during operation.

 h the exception of pagination.

which can be solved using off-the-shelf optimization solvers. Note that the microgrids formation optimization in (20)–(26) is an one-shot decision making problem at the time of restoration, but this formulation can also be used for the following time periods, i.e., at each time the updated system status information is obtained and the optimization is conducted to get the updated microgrids formation and DGs dispatch. It can also be extended to a receding horizon based optimization if the forecast of system status information can be achieved, while the computational complexity in this case will be higher.

IV. Distributed Multiagent Coordination for Global Information Discovery

We design the global information discovery scheme to get the input parameters for the microgrid formation optimization defined in (20)–(26) via a distributed multiagent coordination, as shown in Fig. 2. Each local agent (LA) represents an individual device (e.g., a switch on the line or a node controller) or a group of devices, by setting up communication links (e.g., wireless links) between the LA and devices. The LAs only have a limited computation capability and local communication functions. The regional agent (RA) has an enhanced computation capability to solve the MILP problem defined in (20)–(26). There are several RAs which can be installed at the nodes where the DGs are located to ensure sufficient power supply to perform intensive computation, to compute the microgrids formation optimization to enhance the resilience. Each LA exchanges information with its direct neighboring LAs (and RAs) iteratively, and within a guaranteed number of iterations, the global information can be known to the RAs to perform the optimization. The proposed distributed global information discovery scheme is more resilient than the centralized method when the communication infrastructures are at fault, because the communications between agents can be formed dynamically via wireless links and global information discovery can be achieved by these local communications without the infrastructure support. In addition, multiple RAs geographically distributed provide more resilience than the centralized method in case of the central controller at fault due to the disastrous event.

Note that the communication network can be different from the power distribution network, since it can be formed dynamically after the disaster happens. The topology of the power distribution system is known to the RAs in terms of the ON/OFF status of the switches via the global information discovery. The communication network, on the other hand, can be either static (known to agents) or dynamic (e.g., by forming a wireless *ad hoc* network). We will consider both cases.

Let $\mathcal{M}$ denote the set of LAs in the system, and $M = |\mathcal{M}|$ denotes the number of LAs. Note that $\mathcal{M}$ also includes RAs since each RA also has a module that can conduct the function of a LA. Denote the set of line switches represented by LA m as $\mathcal{L}_m \subset \mathcal{L}$, and the set of load switches represented by LA m as $\mathcal{N}_m \subset \mathcal{N}$. To discover the global information, we design each LA m such that it has four vectors $\boldsymbol{p}_m$, $\boldsymbol{q}_m$, $\boldsymbol{c}_m$, and $\boldsymbol{s}_m$, which track the information exchange for real-power demand, reactive power demand, line switch status, and node switch status, respectively.

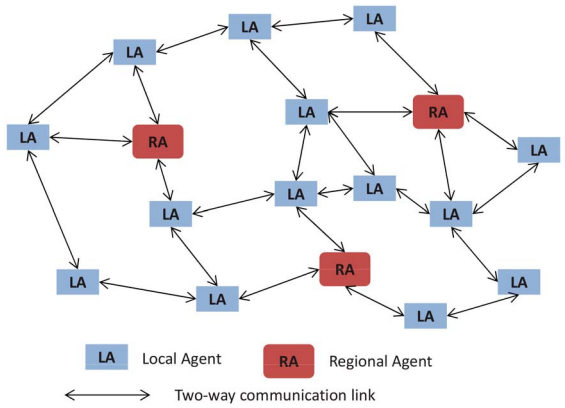

Fig. 2. Multiagent model for information discovery.

Vectors $\boldsymbol{p}_m$ and $\boldsymbol{q}_m$ have a length of N, and the ith position corresponds to the ith node in $\mathcal{N}$. Each LA m initializes its vectors $\boldsymbol{p}_m$ and $\boldsymbol{q}_m$, denoted by $\boldsymbol{p}_m^0$ and $\boldsymbol{q}_m^0$, according to the real and reactive power of the local nodes it represents, and the ith element of $\boldsymbol{p}_m^0$ and $\boldsymbol{q}_m^0$ can be expressed as

$$\boldsymbol{p}_m^0[i] = \begin{cases} Mp_i & i \in \mathcal{N}_m \\ 0 & \text{otherwise} \end{cases} \tag{27}$$

$$\boldsymbol{q}_m^0[i] = \begin{cases} Mq_i & i \in \mathcal{N}_m \\ 0 & \text{otherwise.} \end{cases} \tag{28}$$

The average values of $\boldsymbol{p}_m^0$ and $\boldsymbol{q}_m^0$, denoted by $\bar{\boldsymbol{p}}^0$ and $\bar{\boldsymbol{p}}^0$, respectively, for all LAs $m \in \mathcal{M}$ can be computed as

$$\bar{\boldsymbol{p}}^0 = \frac{1}{M}\sum_{m=1}^{M} \boldsymbol{p}_m^0 = [p_1, p_2, \ldots, p_N]^{\mathrm{T}} \tag{29}$$

$$\bar{\boldsymbol{q}}^0 = \frac{1}{M}\sum_{m=1}^{M} \boldsymbol{q}_m^0 = [q_1, q_2, \ldots, q_N]^{\mathrm{T}} \tag{30}$$

which actually reveal the global information of real and reactive power for all nodes in $\mathcal{N}$.

For the line switches, we define a set $\{1, 0, -1\}$ to denote the different states, in which "1" represents the normal operation state (set of $\mathcal{L}\backslash\{\mathcal{L}_C \cup \mathcal{L}_O\}$), "$-1$" represents the open state (set of $\mathcal{L}_O$), and "0" represents the closed state (set of $\mathcal{L}_C$). The same state definition applies for the node switches. Vector $\boldsymbol{c}_m$ has a length of L, with the ith position corresponding to the ith line in $\mathcal{L}$. Similarly, vector $\boldsymbol{s}_m$ has a length of N, with the ith position corresponding to the ith node in $\mathcal{N}$. Each LA m initializes its vectors $\boldsymbol{c}_m$ and $\boldsymbol{s}_m$, denoted by $\boldsymbol{c}_m^0$ and $\boldsymbol{s}_m^0$, according to the states of the local switches it represents, and the ith element of $\boldsymbol{c}_m^0$ and $\boldsymbol{s}_m^0$ can be expressed as

$$\boldsymbol{c}_m^0[i] = \begin{cases} M & i \in \mathcal{L}_m \cap \mathcal{L} \setminus \{\mathcal{L}_C \cup \mathcal{L}_O\} \\ -M & i \in \mathcal{L}_m \cap \mathcal{L}_O \\ 0 & \text{otherwise} \end{cases} \tag{31}$$

$$\boldsymbol{s}_m^0[i] = \begin{cases} M & i \in \mathcal{N}_m \cap \mathcal{N} \setminus \{\mathcal{N}_C \cup \mathcal{N}_O\} \\ -M & i \in \mathcal{N}_m \cap \mathcal{N}_O \\ 0 & \text{otherwise.} \end{cases} \tag{32}$$

 h the exception of pagination.

The average values of $\boldsymbol{c}_m^0$ and $\boldsymbol{s}_m^0$, denoted by $\bar{\boldsymbol{c}}^0$ and $\bar{\boldsymbol{s}}^0$, respectively, for all agents $m \in \mathcal{M}$ can be computed as

$$\bar{\boldsymbol{c}}^0 = \frac{1}{M}\sum_{m=1}^{M} \boldsymbol{c}_m^0 = \begin{cases} 1 & i \in \mathcal{L} \setminus \{\mathcal{L}_C \cup \mathcal{L}_O\} \\ -1 & i \in \mathcal{L}_O \\ 0 & i \in \mathcal{L}_C \end{cases} \tag{33}$$

$$\bar{\boldsymbol{s}}^0 = \frac{1}{M}\sum_{m=1}^{M} \boldsymbol{s}_m^0 = \begin{cases} 1 & i \in \mathcal{N} \setminus \{\mathcal{N}_C \cup \mathcal{N}_O\} \\ -1 & i \in \mathcal{N}_O \\ 0 & i \in \mathcal{N}_C \end{cases} \tag{34}$$

which reveal the global information of switches' states for all nodes in $\mathcal{N}$ and lines in $\mathcal{L}$.

As discussed above, the average values of the vectors $\boldsymbol{p}_m$, $\boldsymbol{q}_m$, $\boldsymbol{c}_m$, and $\boldsymbol{s}_m$ with proper design of the initialization, reveal all the parameters for the optimization. Inspired by it, the average consensus algorithm [27] can be utilized for this multiagent system to conduct the global information discovery. The algorithm can achieve the average value of all agents (as a consensus agreement) iteratively just by local information exchange. Readers can refer to [27] and references therein for the detailed theoretical analysis of the average consensus algorithm. In this paper, the average consensus algorithm for each LA m can be expressed as

$$\boldsymbol{x}_m^{k+1} = \boldsymbol{x}_m^k + \sum_{r \in \mathcal{R}_m} \varepsilon_{mr} \cdot \left(\boldsymbol{x}_r^k - \boldsymbol{x}_m^k\right) \tag{35}$$

where $\boldsymbol{x}_m^k$ represents the vectors $\boldsymbol{p}_m$, $\boldsymbol{q}_m$, $\boldsymbol{c}_m$, and $\boldsymbol{s}_m$ at step k, and $\mathcal{R}_m$ denotes the set of its direct neighboring LAs. ε_{mr} is the step size for information exchange between LAs m and r. With proper design of step size ε_{mr}, the value of $\boldsymbol{x}_m^k$ will converge to the average of their initialized values,[3] i.e., $\boldsymbol{x}_m^k \to \bar{\boldsymbol{x}}_m = (1/M)\sum_{m=1}^{M} \boldsymbol{x}_m^0$, with given accuracy after a certain number of iterations which is determined by the termination condition. In other words, all LAs, including the RAs, will get the global parameters of real and reactive power demands, line switches' status, and node switches' status.[4] The RAs can then solve the microgrids formation optimization shown in (20)–(26). The solutions in terms of actions (e.g., open or closed) of normal operational switches and outputs of DGs will be broadcast to all LAs, and corresponding actions will be taken to form K self-adequate microgrids energized by DGs.

For the design of step size ε_{mr}, we consider two scenarios.

1) The communication network is time-invariant and network topology is known to each LA.
2) The communication network is dynamic and network topology is not known to each LA.

For the first scenario, the convergence of the average consensus algorithm in (35) is related to the eigenvalue of the Laplacian matrix representing the communication network, which has been studied extensively in the literature (see [27]–[29], and reference therein). As shown in [29], the minimum convergence time is obtained for a constant step size $\varepsilon = 2/[\lambda_2(\mathbf{L}) + \lambda_M(\mathbf{L})]$, where $\lambda_i(\mathbf{L})$ is the ith largest eigenvalue of the graph Laplacian matrix $\mathbf{L}$. With regard to convergence speed, Olfati-Saber *et al.* [27] showed that a discrete-time consensus is globally exponentially reached with a speed that is faster than or equal to $\kappa_2 = 1 - \varepsilon\lambda_2(\mathbf{L})$. These convergence features help in designing the network topology to achieve a better tradeoff between the infrastructure cost and the convergence rate.

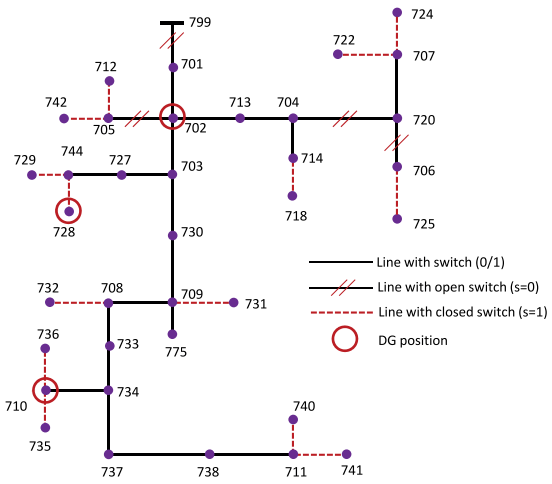

Fig. 3. IEEE 37-node test system with three DGs installed.

However, due to the natural disaster, the communication network may be dynamic; thus the network topology is unknown to each LA to design the optimal step size ε. In this case, step size should be designed based on local connectivity information, i.e., ε_{mr}. In [20] and [30], an improved Metropolis–Hastings method was proposed to adapt to changes of system configuration as

$$\varepsilon_{mr} = \begin{cases} \frac{1}{\max(n_m, n_r)+1} & r \in \mathcal{R}_m \\ 1 - \sum_{r \in \mathcal{R}_m} \frac{1}{\max(n_m, n_r)+1} & m = r \\ 0 & \text{otherwise} \end{cases} \tag{36}$$

where n_m denotes the degree of node (LA) m for the undirected graph representing the communication network. With this method, the step size can be obtained locally to achieve the average consensus, i.e., the global information as input for the MILP optimization.

V. Numerical Results

In this section, we validate our microgrids formation scheme via two modified IEEE radial distribution system test networks, i.e., IEEE 37-node feeder test network [31] and IEEE 123-node feeder test network [32], based on per-phase analysis. CPLEX 12.4 is used to solve the MILP microgrid formation problem. MATLAB 2009a is used to formulate the model and link the CPLEX solver. The simulation environment is of Intel Core i5-3210M 2.5 GHz with 4 GB memory.

A. Case Study I: IEEE 37-Node Feeder System

In this 37-node system, three DGs are assumed to be installed at three nodes (702, 710, 728). Four line switches

[3]We assume that the communication network is connected and two-way communication exists for each link, which guarantees the convergence of the average consensus algorithm in (35).

[4]Note that the final iteration value $\boldsymbol{x}_m^k$ of the switch states (i.e., $\boldsymbol{c}_m^k$ and $\boldsymbol{s}_m^k$) may not converge to the exact integer values (e.g., 0, −1, and 1) due to the iteration termination condition, i.e., the iteration will stop if convergence deviation is less than a tolerance ζ. But with a proper termination tolerance ζ (e.g., $\zeta = 10^{-3}$), the rounding results of $\boldsymbol{x}_m^k$ (to nearest integer) can always give the correct integer values.

 h the exception of pagination.

TABLE I
PARAMETERS FOR DGS

DG	Node position	P (kW)	Q (kVar)
1	702	252.53	46.31
2	728	120.42	171.72
3	710	202.99	197.48

TABLE II
PARAMETERS FOR THE LOAD AT EACH NODE

Node	p (kW)	q (kVar)	Weight	Status (s)
701	30.40	5.09	3.32	0/1
702	18.61	23.60	2.89	0/1
703	38.84	5.76	1.07	0/1
704	26.39	18.40	9.11	0/1
705	12.58	19.25	7.06	0/1
706	29.58	9.90	2.66	0
707	31.09	21.79	3.87	0/1
708	22.57	15.65	6.06	0/1
709	43.08	8.82	4.47	0/1
710	12.57	8.45	7.05	0/1
711	48.23	7.13	8.59	0/1
712	21.06	25.36	4.84	0/1
713	37.61	26.48	9.09	0/1
714	31.51	11.29	4.21	0/1
718	18.89	29.20	3.11	0/1
720	12.17	18.96	6.74	0/1
722	15.36	21.26	9.29	0/1
724	29.37	4.35	2.50	0/1
725	33.82	7.55	6.06	1
727	43.90	14.81	5.12	0/1
728	41.18	7.45	2.95	0/1
729	35.71	3.51	7.57	1
730	43.98	4.07	5.19	0/1
731	24.38	16.95	7.50	0/1
732	48.50	12.72	8.80	0/1
733	5.98	25.31	1.79	0/1
734	7.49	4.80	2.99	0/1
735	12.45	13.76	6.96	0/1
736	35.12	19.28	7.09	0/1
737	11.03	12.74	5.82	0/1
738	46.84	22.32	7.47	0
740	7.41	15.54	2.93	0/1
741	31.86	22.34	4.49	1
742	12.73	24.77	7.19	0/1
744	19.04	7.71	3.23	0/1
775	40.60	28.64	2.48	0/1
799	5.27	19.39	1.21	0

are in open status (at fault) as a result of the disastrous event, as shown in Fig. 3. The line switches that are in closed status are denoted by the dashed line in Fig. 3. The real and reactive power capacity of the three DGs are generated randomly as shown in Table I, and the real and reactive power demand of load at each node as well as its weight are generated randomly as shown in Table II. Note that in practice, how the values of weights are chosen is a complicated problem and many aspects should be considered. Since the focus of the case studies is to validate the microgrids formation optimization proposed, the method to determine the priority weights w_i is out of the scope of this paper. The status of switches for each node are shown in Table II, with 0 indicating open status, 1 indicating closed status, and "0/1" indicating switchable status.

Fig. 4 shows two examples of the convergence results for the multiagent coordination using the average consensus algorithm with a step size suitable for dynamic topology in (36).

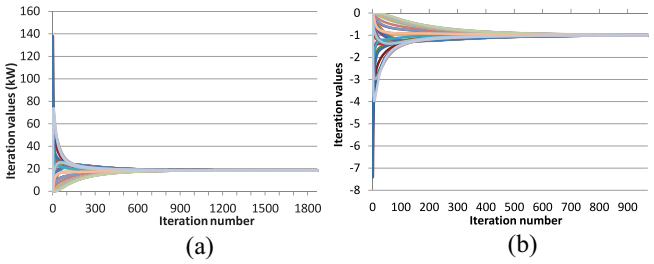

Fig. 4. Examples of convergence results of the multiagent coordination for global information discovery. (a) Convergence of real power of node 702 with 18.61 kW. (b) Convergence of switch status of line (702, 705) with open status.

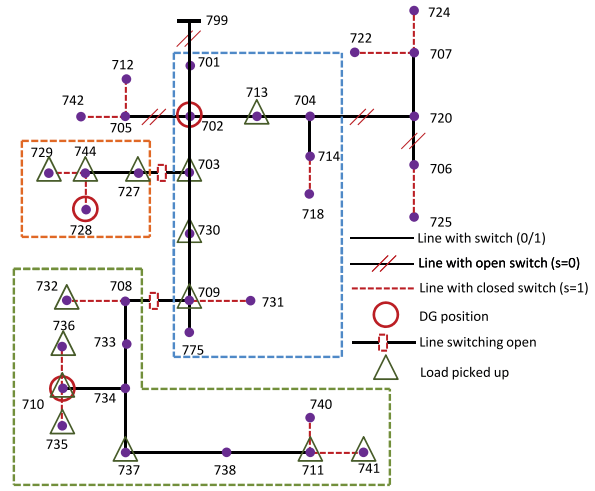

Fig. 5. Microgrids formation results for IEEE 37-node test system, with each microgrid energized by a DG.

In these examples, we assume that the network topology of LAs is the same as that of the distribution network, and each LA represents one line switch and one node switch, i.e., the total number of agents is N. In Fig. 4(a), with proper initialized demand values set according to (27), all LAs, including RAs, finally reach agreement of 18.61 kW, which is the real-power demand of node 702. In Fig. 4(b), with proper initialized switch status values set according to (31), all LAs, including RAs, finally reach the consensus of -1, representing the open status of the switch at the line (702, 705). Other values can also be obtained at each LA and RA in the same way, and the RAs solve the MILP problem and then broadcast the ON/OFF decisions of these switches and generation values of DGs to each LA to realize the microgrids formation.

Note that each LA can represent several switches so that the number of agents will be less than N and the convergence will be faster. The convergence is guaranteed if the communication network of the agents is connected. Also in the test case, the communication network is of radial topology, but if more connections can be made among agents (e.g., forming a mesh network), the convergence time will be improved since the larger $\lambda_2(\mathbf{L})$ will increase the convergence speed [27]. The convergence examples here are illustrations of the multiagent coordination scheme. The actual communication network design, however, should consider several practical

 h the exception of pagination.

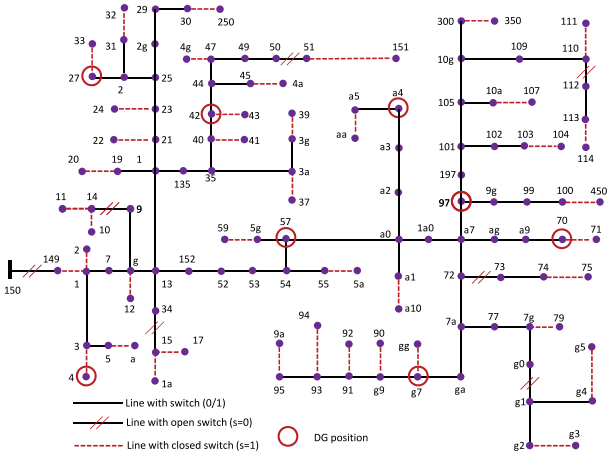

Fig. 6. IEEE 123-node test system with eight DGs installed.

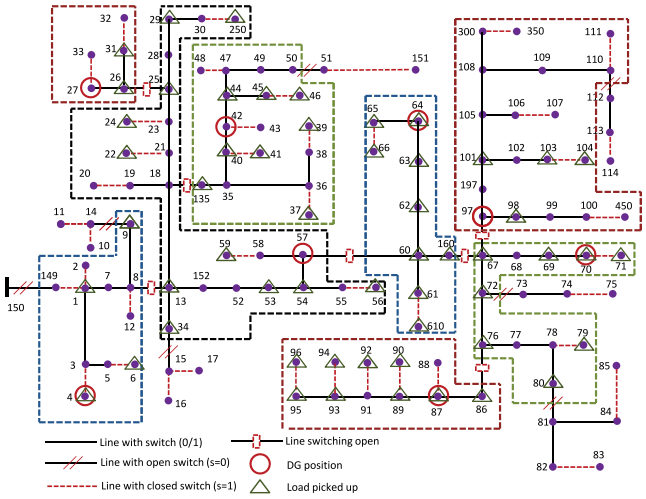

Fig. 7. Microgrids formation results for IEEE 123-node test system, with each microgrid energized by a DG.

aspects such as communication ranges, battery capacity to support the communication module, the time requirements for the global information discovery, and so forth, which are out of the scope of this paper.

Fig. 5 shows the microgrid formation optimization results. Three microgrids are formed by opening/closing line switches, and each one is energized by one DG. The voltage of nodes are within the range specified. The loads picked up, labeled by triangles in Fig. 5, are achieved by opening/closing node switches. The computation time for the MILP problem is 0.265 s.

B. Case Study II: IEEE 123-Node Feeder System

Fig. 6 shows the IEEE 123-node system with eight DGs installed at eight nodes. There are seven line switches in open status (at fault) as a result of the disastrous event, as shown in Fig. 6, and the line switches in closed status are denoted by the dashed line as shown in Fig. 6. Similar to the previous case study, the real and reactive power capacity of the DGs are randomly generated. The real and reactive power demand of load at each node, as well as its weight, are generated randomly. Among the node switches, six nodes switches are randomly chosen as in open status and six nodes switches are randomly chosen as in closed status, while other switches are in normal switchable status. Due to space limitation, these values are not shown in this paper.

Fig. 7 shows the microgrids formation optimization results for the 123-node test system. Eight microgrids are formed separately by opening/closing line switches, and each one is energized by one DG. The loads are picked up by closing certain node switches, labeled by triangles in Fig. 7. The computation time for the MILP problem is 2.402 s.

VI. Conclusion

In this paper, we proposed a microgrid formation mechanism to restore critical loads after a major fault happens at the main grid as a result of a natural disaster, by exploiting the DGs and automatic remotely controlled switches which are being installed more and more by utilities. A MILP problem was formulated to maximize the total prioritized loads restored while satisfying self-adequacy and operation constraints of each microgrid. A distributed multiagent coordination scheme was designed to achieve global information discovery via only local communications, which is suitable for resilient communication requirements after a natural disaster. The formed microgrids serve as starting points for further power quality control and can be connected to form a larger microgrid before the completion of main grid restoration.

References

[1] L. Che, M. Khodayar, and M. Shahidehpour, "Only connect: Microgrids for distribution system restoration," *IEEE Power Energy Mag.*, vol. 12, no. 1, pp. 70–81, Jan./Feb. 2014.

[2] R. J. Campbell, "Weather-related power outages and electric system resiliency," Congr. Res. Serv., Washington, DC, USA, Tech. Rep. R42696, Aug. 2012. [Online]. Available: http://www.fas.org/sgp/crs/misc/R42696.pdf

[3] President's Council of Economic Advisers and the U.S. Department of Energy's Office of Electricity and Energy Reliability, "Economic benefits of increasing electric grid resilience to weather outages," Executive Office of the President, U.S. Dept. Energy, Washington, DC, USA, Tech. Rep., Aug. 2013. [Online]. Available: http://energy.gov/sites/prod/files/2013/08/f2/Grid%20Resiliency%20Report_FINAL.pdf

[4] C. C. Liu, S. J. Lee, and S. S. Venkata, "An expert system operational aid for restoration and loss reduction of distribution systems," *IEEE Trans. Power Syst.*, vol. 3, no. 2, pp. 619–626, May 1988.

[5] C. S. Chen, C. H. Lin, and H. Y. Tsai, "A rule-based expert system with colored Petri net models for distribution system service restoration," *IEEE Trans. Power Syst.*, vol. 17, no. 4, pp. 1073–1080, Nov. 2002.

[6] S. I. Lim, S. J. Lee, M. S. Choi, D. J. Lim, and B. N. Ha, "Service restoration methodology for multiple fault case in distribution systems," *IEEE Trans. Power Syst.*, vol. 21, no. 4, pp. 1638–1644, Nov. 2006.

[7] S. J. Lee, S. I. Lim, and B.-S. Ahn, "Service restoration of primary distribution systems based on fuzzy evaluation of multi-criteria," *IEEE Trans. Power Syst.*, vol. 13, no. 3, pp. 1156–1163, Aug. 1998.

[8] J. M. Solanki, S. Khushalani, and N. N. Schulz, "A multi-agent solution to distribution systems restoration," *IEEE Trans. Power Syst.*, vol. 22, no. 3, pp. 1026–1034, Aug. 2007.

[9] C. P. Nguyen and A. J. Flueck, "Agent based restoration with distributed energy storage support in smart grids," *IEEE Trans. Smart Grid*, vol. 3, no. 2, pp. 1029–1038, Jun. 2012.

[10] A. L. Morelato and A. Monticelli, "Heuristic search approach to distribution system restoration," *IEEE Trans. Power Del.*, vol. 4, no. 4, pp. 2235–2241, Oct. 1989.

[11] S. Khushalani, J. M. Solanki, and N. N. Schulz, "Optimized restoration of unbalanced distribution systems," *IEEE Trans. Power Del.*, vol. 22, no. 2, pp. 624–630, May 2007.

 h the exception of pagination.

[12] T. T. H. Pham, Y. Besanger, and N. Hadjsaid, "New challenges in power system restoration with large scale of dispersed generation insertion," *IEEE Trans. Power Syst.*, vol. 24, no. 1, pp. 398–406, Feb. 2009.

[13] R. B. Hickey, *Electrical Construction Databook*. New York, NY, USA: McGraw Hill, 2002.

[14] SmartGrid.gov. (May 2014). *Recovery Act Smart Grid Programs: Project Information*. [Online]. Available: https://www.smartgrid.gov/recovery_act/project_information

[15] C. L. Moreira, F. O. Resende, and J. A. P. Lopes, "Using low voltage microgrids for service restoration," *IEEE Trans. Power Syst.*, vol. 22, no. 1, pp. 395–403, Feb. 2007.

[16] A. Castillo, "Microgrid provision of blackstart in disaster recovery for power system restoration," in *Proc. IEEE SmartGridComm*, Vancouver, BC, Canada, 2013, pp. 534–539.

[17] E. Zare and M. Shahabi, "Microgrid restoration after major faults in main grid with automatic and constant time switching," *Int. J. Intell. Syst. Appl.*, vol. 5, no. 10, pp. 50–58, Sep. 2013.

[18] J. Li, X. Y. Ma, C. C. Liu, and K. P. Schneider, "Distribution system restoration with microgrids using spanning tree search," *IEEE Trans. Power Syst.*, vol. 29, no. 6, pp. 3021–3029, Nov. 2014.

[19] Z. Wang and J. Wang, "Self-healing resilient distribution systems based on sectionalization into microgrids," *IEEE Trans. Power Syst.*, to be published.

[20] Y. Xu and W. Liu, "Novel multiagent based load restoration algorithm for microgrids," *IEEE Trans. Smart Grid*, vol. 2, no. 1, pp. 152–161, Mar. 2011.

[21] G. T. Heydt, "The next generation of power distribution systems," *IEEE Trans. Smart Grid*, vol. 7, no. 4, pp. 66–76, Nov. 2012.

[22] A. M. Cuomo, R. L. Kauffman, J. B. Rhodes, A. Zibelman, and J. M. Hauer, "Microgrids for critical facility resiliency in New York state," New York State Energy Res. Develop. Authority, Albany, NY, USA, Tech. Rep. 14-36s, Dec. 2014.

[23] A. R. Hopper *et al.*, "Maryland resiliency through microgrid task force report," Maryland Energy Admin., Annapolis, MD, USA, Tech. Rep., Jun. 2014.

[24] Avista Utilities. (Mar. 2015). *Avista Utilities Spokane Smart Circuit Project*. [Online]. Available: https://www.avistautilities.com/inside/resources/smartgrid/smartcircuits/Pages/default.aspx

[25] M. E. Baran and F. F. Wu, "Optimal capacitor placement on radial distribution systems," *IEEE Trans. Power Del.*, vol. 4, no. 1, pp. 725–734, Jan. 1989.

[26] H. Yeh, D. F. Gayme, and S. H. Low, "Adaptive VAR control for distribution circuits with photovoltaic generators," *IEEE Trans. Power Syst.*, vol. 27, no. 3, pp. 1656–1663, Aug. 2012.

[27] R. Olfati-Saber, J. A. Fax, and R. M. Murray, "Consensus and cooperation in networked multi-agent systems," *Proc. IEEE*, vol. 95, no. 1, pp. 215–233, Jan. 2007.

[28] R. Olfati-Saber and R. M. Murray, "Consensus problems in networks of agents with switching topology and time-delays," *IEEE Trans. Autom. Control*, vol. 49, no. 9, pp. 1520–1533, Sep. 2004.

[29] L. Xiao and S. Boyd, "Fast linear iterations for distributed averaging," *Syst. Control Lett.*, vol. 53, no. 1, pp. 65–78, 2004.

[30] L. Xiao, S. Boyd, and S. Kim, "Distributed average consensus with least-mean-square deviation," *J. Parallel Distrib. Comput.*, vol. 67, no. 1, pp. 33–46, 2007.

[31] IEEE PES Power System Analysis, Computing, and Economics Committee. (Feb. 2014). *IEEE 37 Node Test Feeder*. [Online]. Available: http://ewh.ieee.org/soc/pes/dsacom/testfeeders/feeder37.zip

[32] IEEE PES Power System Analysis, Computing, and Economics Committee. (Feb. 2014). *IEEE 123 Node Test Feeder*. [Online]. Available: http://ewh.ieee.org/soc/pes/dsacom/testfeeders/feeder123.zip

Chen Chen (M'13) received the B.S. and M.S. degrees in electrical engineering from Xi'an Jiaotong University, Xi'an, China, in 2006 and 2009, respectively, and the Ph.D. degree in electrical engineering from Lehigh University, Bethlehem, PA, USA, in 2013.

He is currently a Postdoctoral Researcher with the Energy Systems Division, Argonne National Laboratory, Argonne, IL, USA. His current research interests include optimization, communications, and signal processing for smart electricity systems.

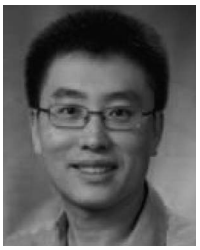

Jianhui Wang (M'07–SM'12) received the Ph.D. degree in electrical engineering from the Illinois Institute of Technology, Chicago, IL, USA, in 2007.

Currently, he is the Section Lead for Advanced Power Grid Modeling at the Energy Systems Division, Argonne National Laboratory, Argonne, IL. He is an Affiliate Professor with Auburn University, Auburn, AL, USA, and an Adjunct Professor with the University of Notre Dame, Notre Dame, IN, USA.

Dr. Wang is the Editor-in-Chief of the IEEE TRANSACTIONS ON SMART GRID and a Distinguished Lecturer of the IEEE POWER AND ENERGY SOCIETY LETTERS, an Editor of the IEEE TRANSACTIONS ON POWER SYSTEMS, an Associate Editor of the *Journal of Energy Engineering*, and an Editorial Board Member of *Applied Energy*. He is an IEEE Power and Energy Society (PES) Distinguished Lecturer. He is the Secretary of the IEEE PES Power System Operations Committee. He was the Chair of the IEEE PES Power System Operation Methods Subcommittee for six years.

Feng Qiu (M'14) received the B.S. and M.S. degrees in automation from the Huazhong University of Science and Technology, Wuhan, China, in 2000 and 2003, respectively, and the Ph.D. degree in industrial and systems engineering with the Georgia Institute of Technology, Atlanta, GA, USA, in 2013.

He was an Operations Research Analyst with Shanghai Firsttech, Shanghai, China. He is currently a Postdoctoral Researcher with the Energy Systems Division, Argonne National Laboratory, Argonne, IL, USA. His current research interests include optimization in power system operations, electricity markets, and power grid resilience.

Dongbo Zhao (S'10–M'14) received the B.S. degree from Tsinghua University, Beijing, China, in 2008, and the M.S. degree from Texas A&M University, College Station, TX, USA, in 2010, both in electrical engineering.

He has worked with ABB Inc., US Corporate Research Center, Raleigh, NC, USA, from 2010 to 2011. He is currently with Eaton Corporation, Eden Prairie, MN, USA. His current research interests include power system control, protection, reliability analysis, transmission and distribution automation, and electric market optimization.